Available online at www.sciencedirect.com

ScienceDirect

IFAC PapersOnLine 50-1 (2017) 5788–5793

A 3D Decentralized Guidance and Control System for a Swarm of Multi-Copters

Gaetano Tartaglione * **Marco Ariola** * **Egidio D'Amato** ** **Pierluigi Salvo Rossi** ***

* *Department of Engineering, University of Naples "Parthenope", Napoli, Italy (e-mail: {gaetano.tartaglione,marco.ariola}@uniparthenope.it)*

** *Department of Industrial and Information Engineering, University of Campania "L. Vanvitelli", Aversa, Italy (e-mail: egidio.damato@unina.it)*

*** *Department of Electronics and Telecommunications, Norwegian University of Science and Technology, Trondheim, Norway (email: salvorossi@iet.ntnu.no)*

Abstract: In this paper we present a decentralized real-time system for the guidance and control of a swarm of multi-copters in a 3D environment. A hierarchical architecture is proposed for trajectory planning and tracking based on the control of the multi-copter attitude and velocity. The guidance module generates the reference trajectory as a sequence of way-points, obtained as solution to a constrained optimization problem. The tracking trajectory module is based on a distributed and robust Model Predictive Control (MPC) technique. Finally, a cascaded PID controller is used for attitude and velocity control. To test the proposed scheme, we consider a cooperative load transport problem in which a suspended load is linked by wires to the multi-copters. Numerical simulations of realistic scenarios are presented. The results are encouraging, thus making the proposed system an appealing candidate for a wide range of applications.

Keywords: trajectory tracking and path following, decentralized control systems, multi-vehicle systems.

1. INTRODUCTION

In the recent years, multi-agent cooperative control has gained significant interest within the control research community (Murray, 2007; Cao et al., 2012). The diffusion of Unmanned Aerial Vehicles (UAVs) has extended the interest to the aeronautic research community where the main focus is the design of autonomous multi-vehicle systems to be used for several purposes ranging from surveillance to transportation, including monitoring, exploration, search and rescue. In this framework, guidance and control must account for formation flight, whose main goal is to achieve a desired group formation shape while controlling the overall behavior of the group.

Many of the control scheme designed for formation flight are based on a decomposition hierarchic method (Farina et al., 2015; Ariola et al., 2016): first a path planning problem is solved taking into account the mission goal, the coordination among aircrafts and the collision avoidance, then a controller is designed to track the reference trajectory.

Lot of algorithms for path planning and coordination problems have been developed and evaluated in terms of optimality (length and flying time), computational complexity and approximation of the operating scenario. In particular, path planning and coordination problems in formation flight have been solved by map discretization method and graph search algorithm (Pascarella et al., 2015); artificial potential field approach (Paul et al., 2008); Voronoi tessellation algorithm (Lee, 2015); consensus approach (Dong et al., 2014); constrained optimization problems approach (Farina et al., 2015).

Various control techniques have been proposed for the multi-copter tracking trajectory problem and evaluated in terms of tracking error, control power and robustness requirement. In particular, tracking trajectory in formation flight has been tackled using PID controllers (Luo et al., 2014), the geometric control approach (Lee, 2014), the passivity-based approach (Bai et al., 2011), distributed kinematic control law (Klausen et al., 2014), the backstepping technique (Klausen et al., 2015), the MPC technique (Farina et al., 2014), nonlinear dynamic inversion technique (D'Amato et al., 2015).

In this paper, we present a decentralized real-time guidance and control system for the formation flight of a swarm of multi-copters. In particular, the coordination problem is approached using the virtual structure technique (Lewis and Tan, 1997); the 3D path planning problem is solved using a constrained optimization approach; tracking of the reference trajectory is guaranteed by a controller designed with the MPC technique; finally cascaded PID controllers are used for velocity and attitude control.

2405-8963 © 2017, IFAC (International Federation of Automatic Control) Hosting by Elsevier Ltd. All rights reserved.
Peer review under responsibility of International Federation of Automatic Control.
10.1016/j.ifacol.2017.08.424

To obtain coordination and decentralize the guidance module, each multi-copter computes its own reference trajectory using a constrained optimization approach and the virtual structure technique. The reference trajectory is expressed as a sequence of way-points, which are the solution of a sequence of constrained optimization problems, solved through a decentralized approach.

The trajectory tracking module is based on a decentralized and robust MPC algorithm (Farina et al., 2014). At each discrete time instant, each multi-copter obtains the control signals as the solution to a constrained optimization problem, using a receding horizon strategy. The optimization problem is defined assuming the knowledge of a reference trajectory and a prediction of the system behavior over a future horizon. This MPC algorithm allows us to take into account the presence of control input saturations, the requirement of robustness and sustainable computational cost for a real-time application.

To validate the proposed scheme, we consider a cooperative load transport problem in which a suspended load is linked by wires to the multi-copters. In particular, a simulator has been developed using the 6DoF model for the multi-copters dynamic (Stevens and Lewis, 2003), while the Udwadia-Kalaba equation is exploited to obtain the constraints of the interconnected system (Udwadia and Phohomsiri, 2007).

The paper is organized as follows. Section 2 presents the architecture of the guidance and control system. Section 3 describes the optimization problem for computing the leader reference trajectory, while Section 4 illustrates the MPC technique implementation. In Section 5, we describe the simulator of the multi-body slung-load system, and show the numerical results of the simulation performed for system testing and validation. Finally, in Section 6 we draw some conclusions.

Notation In the sequel by the symbol $\|\cdot\|$ we will denote the Euclidean norm, whereas by $\|\cdot\|_T$ we will denote the Euclidean norm weighted by the positive definite matrix T. By $A \succ 0$ we mean that each element of the matrix A is greater than 0. The symbol $\wedge$ denotes the cross product between two vectors. The symbol $\times$ denotes the Cartesian product between two sets. The symbols $\oplus$ and $\ominus$ denote respectively the Minkowski sum and the Pontryagin difference (Nguyen, 2014). The symbol $(\cdot)^+$ denotes the Moore-Penrose Pseudo inverse (De Falco et al., 2009). With $\mathscr{C}^n(a)$ we denote the set obtained by $[-a;a]_1 \times [-a;a]_2 \times ... [-a;a]_n$; with I_n we denote the identity matrix of order n and with $0_{m\times n}$ we denote the m-by-n matrix of zeros. Finally given a vector v, diag(v) indicates a diagonal matrix whose diagonal is the vector v.

2. GUIDANCE AND CONTROL SYSTEM ARCHITECTURE

The proposed control scheme for the formation flight of a swarm of M multi-copters has been designed using a decentralized approach. In particular, for each multi-copter we consider an on-board guidance and control system composed by three modules. As shown in Fig. 1 the modules, connected by a hierarchical architecture, perform the following tasks: (i) generation of the reference trajectory; (ii) computation of the reference speeds needed to track the reference trajectory; (iii) speed and attitude control.

The planning trajectory module implements the constrained optimization approach and the virtual structure technique. The sampling time is Δt, the input parameters are the final position of the virtual leader $\tilde{p}^{[goal]}$ and the boundary of the no-fly zones, while the output is the reference way-point of the i-th multi-copter $\tilde{p}^{[i]}_{t+N-1} = \left[\tilde{x}^{[i]}_{t+N-1}\ \tilde{y}^{[i]}_{t+N-1}\ \tilde{z}^{[i]}_{t+N-1}\right]^T$. To implement a receding horizon strategy, at each discrete time instant t the module computes the way-point at $t+N-1$, where N is the length of the optimization horizon of the MPC technique. The point $\tilde{p}^{[i]}_{t+N-1}$ is obtained from the virtual leader way-point $\tilde{p}^{[leader]}_{t+N-1}$ assuming that the virtual structure is known, as

$$\tilde{p}^{[i]}_{t+N-1} = \tilde{p}^{[leader]}_{t+N-1} + l^{[i]} \begin{bmatrix} \sin\nu^{[i]}\cos\alpha^{[i]} \\ \sin\nu^{[i]}\sin\alpha^{[i]} \\ -\cos\nu^{[i]} \end{bmatrix}, \qquad (1)$$

where the distance $l^{[i]}$, the elevation angle $\nu^{[i]}$ and the azimuth angle $\alpha^{[i]}$ define the virtual structure as shown in Fig. 2. The leader way-point is computed as the solution of the constrained optimization problem described in Section 3.2. The decentralized approach is implemented defining the same constrained optimization problem for each multi-copter, which share their own solution with the other UAVs. In the guidance module, we introduce the leader reference trajectory decision sub-module to compare the cost function of all the solutions and find the best one; then the way-point obtained as output of this sub-module is the same for all the multi-copters. In this paper, we assume that the UAVs are linked through an ideal (instantaneous and error-free) communication network.

The tracking trajectory module implements a robust MPC technique. The sampling time is Δt, the input parameter is the multi-copter way-point $\tilde{p}^{[i]}_{t+N-1}$, while the outputs are the reference speeds vector $\tilde{V}^{[i]}_t = \left[\tilde{V}^{[i]}_{x_t}\ \tilde{V}^{[i]}_{y_t}\ \tilde{V}^{[i]}_{z_t}\right]^T$. The MPC technique allows us to compute the reference acceleration $\tilde{a}^{[i]}_t = \left[\tilde{a}^{[i]}_{x_t}\ \tilde{a}^{[i]}_{y_t}\ \tilde{a}^{[i]}_{z_t}\right]^T$ and then to obtain the reference speeds. To define the MPC optimization problem we introduce the reference state/input sub-module to compute the reference states $\tilde{x}^{[i]}_{\{t,\ldots,t+N-1\}}$ and input $\tilde{u}^{[i]}_{\{t,\ldots,t+N-2\}}$ from the sequence of the way-points.

The speed and attitude control module is carried out by means of PID controllers. The sampling time is Δt_{inner}, with $\Delta t_{inner} < \Delta t$, the input parameters are the reference speeds, while the outputs are multi-copter motors speed vector $\omega^{[i]}_t$. The PID controllers are used to obtain roll $(\tilde{\phi})$ and pitch $(\tilde{\theta})$ reference angles. Then, an attitude and vertical speed controller is designed using the classical approach described in Mahony et al. (2012).

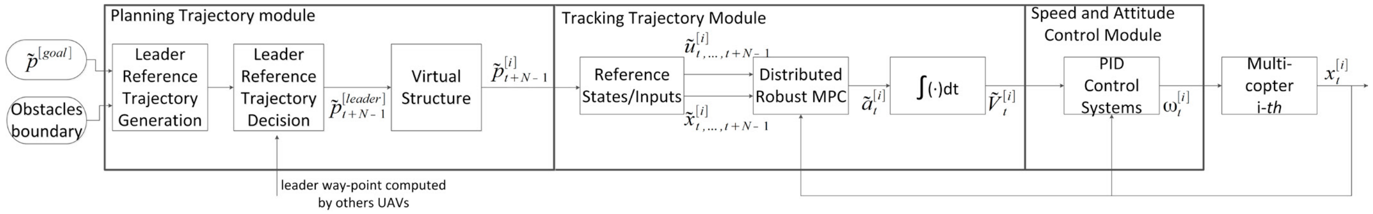
$\tilde{p}^{[goal]}$
Obstacles boundary
Planning Trajectory module
Leader Reference Trajectory Generation
Leader Reference Trajectory Decision
$\tilde{p}^{[leader]}_{t+N-1}$
Virtual Structure
$\tilde{p}^{[i]}_{t+N-1}$
leader way-point computed by others UAVs
Tracking Trajectory Module
Reference States/Inputs
$\tilde{u}^{[i]}_{t,\dots,t+N-1}$
$\tilde{x}^{[i]}_{t,\dots,t+N-1}$
Distributed Robust MPC
$\tilde{a}^{[i]}_t$
$\int(\cdot)dt$
$\tilde{V}^{[i]}_t$
Speed and Attitude Control Module
PID Control Systems
$\omega^{[i]}_t$
Multi-copter i-th
$x^{[i]}_t$

Fig. 1. Guidance and Control System Architecture.

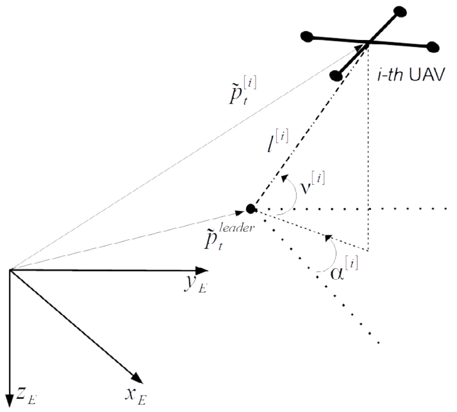

Fig. 2. Virtual structure geometry.

3. GENERATION OF THE LEADER REFERENCE TRAJECTORY

3.1 Way-point generation

The leader reference trajectory is defined as a sequence of way-points. Each way-point is obtained as solution of a constrained optimization problem. To obtain feasible trajectories for each UAV, operational constrains about multi-copters positions are taken into account in the optimization problem considering for $i = 1, ..., M$ the relation

$$\tilde{p}^{[i]}_{t+N-1} = \begin{bmatrix} 1 & 0 & 0 & l^{[i]}\sin\nu^{[i]}\cos\alpha^{[i]} \\ 0 & 1 & 0 & l^{[i]}\sin\nu^{[i]}\sin\alpha^{[i]} \\ 0 & 0 & 1 & -l^{[i]}\cos\nu^{[i]} \end{bmatrix} \begin{bmatrix} \tilde{p}^{[leader]}_{t+N-1} \\ 1 \end{bmatrix}. \quad (2)$$

To minimize the distance from the final point, at each discrete time instant the guidance module solves the following optimization problem

$$\min_{\tilde{p}^{[leader]}_{t+N-1}} \beta \left\| \tilde{p}^{[leader]}_{t+N-1} - \tilde{p}^{[leader]}_{t+N-2} \right\|^2 + \left\| \tilde{p}^{[leader]}_{t+N-1} - p^{[goal]} \right\|^2_T, \quad (3)$$

subject to obstacle avoidance constraints and to

$$\tilde{p}^{[leader]}_{t+N-1} \in \mathscr{B}_{t+N-1}, \quad (4a)$$

$$\tilde{p}^{[i]}_{t+N-1} \in \mathbb{Z} \quad i = 1, ..., M. \quad (4b)$$

In particular, the quadratic cost function (3) is calculated from the last way-point $\tilde{p}^{[leader]}_{t+N-2}$, the final position $\tilde{p}^{[goal]}$ and the weights T and β, with $T \succ \beta I_3$.

To obtain coordination, the obstacle avoidance strategy allows multi-copters to avoid the collisions without breaking up the formation. In particular, the leader way-point must guarantee that all the multi-copters way-points are outside the safety 3D no-fly zones surrounding the obstacles. The no-fly zone is defined through the safety distance d_{safety}

$$d_{safety} = \delta + d_{UAV}, \quad (5)$$

where the distance δ takes into account the maximum uncertainty about the UAVs position and it is estimated using the algorithm in Farina et al. (2015), and d_{UAV} is the radius of the sphere surrounding the multi-copters body. The obstacle avoidance constraints are formulated in the Section 3.2.

The constraint (4a) allows us to control the norm of the UAVs cruise speed. In particular, the set $\mathscr{B}_{t+N-1}$ is bounded by a sphere of the center $\tilde{p}^{[leader]}_{t+N-2}$ and radius $d_{cruise} = \Delta t V_{cruise}$.

The constraint (4b) guarantees that the reference states $\tilde{x}^{[i]}_{\{t,\dots,t+N-1\}}$, computed from the reference way-points, define a feasible MPC problem. The set $\mathbb{Z}$ depends on the MPC technique and is computed using the algorithm in Farina et al. (2015).

3.2 Obstacle avoidance constraint

The obstacle avoidance strategy has been formulated in order to obtain linear constraints and it allows us to consider obstacles represented by convex polytopes of whose vertices have known positions. In the sequel, referring to the i-th multi-copter, the h-th obstacle is modeled by the polytope $\mathscr{P}^{[ih]}$ characterized by k faces. In particular, we consider that $\mathscr{P}^{[ih]}$ is inside the set $\mathscr{B}_{t+N-1}$. To avoid collision, we impose

$$d^{[ih]}_j(\tilde{p}^{[i]}_{t+N-1}) > d_{safety} \quad j = 1, ..., k, \quad (6)$$

where $d^{[ih]}_j(\tilde{p}^{[i]}_{t+N-1})$ is the distance between the way-point $\tilde{p}^{[i]}_{t+N-1}$ and the j-the face of the polytope.

To implement condition (6), we consider the operator

$$\begin{aligned} &\rho^{[ih]}_j(\tilde{p}^{[i]}_{t+N-2}) \\ &\quad = -\operatorname{sign}(a^{[h]}_j x^{[obs]} + b^{[h]}_j y^{[obs]} + c^{[h]}_j z^{[obs]} \\ &\quad + 1)\frac{a^{[h]}_j \tilde{x}^{[i]}_{t+N-2} + b^{[h]}_j \tilde{y}^{[i]}_{t+N-2} + c^{[h]}_j \tilde{z}^{[i]}_{t+N-2} + 1}{\sqrt{{a^{[h]}_j}^2 + {b^{[h]}_j}^2 + {c^{[h]}_j}^2}}, \quad (7) \end{aligned}$$

where the point $p^{[obs]} = \begin{bmatrix} x^{[obs]} & y^{[obs]} & z^{[obs]} \end{bmatrix}^T$ is inside the h-th polytope, while the coefficients $a^{[h]}_j$,$b^{[h]}_j$ and $c^{[h]}_j$ define the equation of the plane containing the j-th polytope face. The coefficients $a^{[h]}_j$,$b^{[h]}_j$ and c^{i}_j in (7) are computed solving the linear system defined by the equation

$$a^{[h]}_j x^i_v + b^{[h]}_j y^i_v + c^{[h]}_j z^i_v + 1 = 0\,,$$

for $i = 1, 2, 3$, where $\left[x_v^i \; y_v^i \; z_v^i\right]^T$ are three vertices of the j-th face. For a given couple i, h, a negative value for $\rho_j^{[ih]}(\tilde{p}_{t+N-2}^{[i]})$ means that the distance between the way-point of the multi-copter i and the plane containing the face j is greater than the distance between this plane and any point $p^{[obs]}$ internal to the polytope h. Hence there will certainly be another face of the polytope closer to the way-point, and therefore the face j is discarded. When $\rho_j^{[ih]}(\tilde{p}_{t+N-2}^{[i]})$ is positive, it returns the distance between the way-point and the plane containing the face j of the polytope.

For each multi-copter i and obstacle h we compute $\rho_j^{[ik]}(\tilde{p}_{t+N-2}^{[i])})$ for $j = 1, ..., k$ and we select the index $\bar{j}$ corresponding to the maximum value of $\rho_j^{[ih]}(\tilde{p}_{t+N-2}^{[i]})$ for $j = 1, ..., k$ and we include the following linear inequality in the optimization problem

$$\rho_{\bar{j}}^{[ih]}(\tilde{p}_{t+N-1}^{[i]}) > d_{UAV} + \delta \, . \tag{8}$$

To consider a obstacle with circular cross section, we approximate it with a regular polytope with $r_{obs}^{[hi]}$ faces. In particular, we approximate the circular cross section through the surrounding 2D polytope with $r_{obs}^{[hi]}$ edges. It is worth noting that this approximation is conservative: the approximation error decreases with $r_{obs}^{[hi]}$.

4. TRACKING TRAJECTORY MODULE

The tracking trajectory module implements a robust and decentralized MPC technique to compute the multi-copter control input. Each UAV computes its own control inputs independently from the other multi-copters using the same algorithm, since the coordination problem has already solved by the guidance module.

To implement the MPC algorithm, the tracking module solves a constrained optimization problem at each discrete time instant. The cost and constraint functions are computed from a prediction of the UAV behavior and the reference states and inputs. The sequences of reference states and inputs are calculated from the geometrical reference trajectory by the reference states/inputs sub-module (see Figure 1). The multi-copter behavior is predicted using the dynamic model of a material point in the space.

4.1 MPC predicted states

The dynamic model of a material point in the space can be formulated in terms of the position $[x_E \; y_E \; z_E]^T$ in the inertial earth frame E, the course angle Ψ, the climb angle γ and the linear velocity V as

$$\begin{cases} \dot{x}_E = V \cos\Psi \cos\gamma \\ \dot{y}_E = V \sin\Psi \cos\gamma \\ \dot{z}_E = V \sin\gamma \\ \dot{\Psi} = \omega_1 \\ \dot{\gamma} = \omega_2 \\ \dot{V} = a \end{cases}$$

where the inputs of system are the angular velocities ω_1 and ω_2 and the linear acceleration a.

Extending the 2D procedure in Oriolo et al. (2002), we obtain a linear model of a material point. Letting $\eta_1 = x_E$, $\eta_2 = \dot{x}_E$, $\eta_3 = y_E$, $\eta_4 = \dot{y}_E$, $\eta_5 = z_E$, $\eta_6 = \dot{z}_E$

$$\begin{cases} \dot{\eta}_1 = \eta_2 \\ \dot{\eta}_2 = a\cos\Psi\cos\gamma - V\omega_1 \sin\Psi\cos\gamma - V\omega_2 \sin\Psi\sin\gamma \\ \dot{\eta}_3 = \eta_4 \\ \dot{\eta}_4 = a\sin\Psi\cos\gamma + V\omega_1 \cos\Psi\cos\gamma - V\omega_2 \sin\Psi\sin\gamma \\ \dot{\eta}_5 = \eta_6 \\ \dot{\eta}_6 = \dot{V}\sin\gamma + V\omega_2\cos\gamma \end{cases}$$

and introducing the linear accelerations a_x, a_y and a_z

$$\begin{aligned} a_x &\equiv a\cos\Psi\cos\gamma - V\omega_1 \sin\Psi\cos\gamma - V\omega_2 \sin\Psi\sin\gamma, \\ a_y &\equiv a\sin\Psi\cos\gamma + V\omega_1 \cos\Psi\cos\gamma - V\omega_2 \sin\Psi\sin\gamma, \\ a_z &\equiv \dot{V}\sin\gamma + V\omega_2\cos\gamma, \end{aligned}$$

we obtain a set of three decoupled double integrators. Finally, the discrete time dynamic model is obtained by a Euler discretization with sampling time Δt

$$x_{t+1} = Ax_t + Bu_t + w_t, \tag{9}$$

$$p_{t+1} = Cx_{t+1}, \tag{10}$$

where

$$\begin{aligned} x_t &= \left[\eta_{1_t} \; \eta_{2_t} \; \eta_{3_t} \; \eta_{4_t} \; \eta_{5_t} \; \eta_{6_t}\right]^T \; , \\ u_t &= \left[a_{x_t} \; a_{y_t} \; a_{z_t}\right]^T \; , \quad p_t = \left[x_{E_t} \; y_{E_t} \; z_{E_t}\right]^T \; , \end{aligned}$$

$$A = \begin{bmatrix} 1 & \Delta t & 0 & 0 & 0 & 0 \\ 0 & 1 & 0 & 0 & 0 & 0 \\ 0 & 0 & 1 & \Delta t & 0 & 0 \\ 0 & 0 & 0 & 1 & 0 & 0 \\ 0 & 0 & 0 & 0 & 1 & \Delta t \\ 0 & 0 & 0 & 0 & 0 & 1 \end{bmatrix}, \quad B = \begin{bmatrix} \frac{\Delta t^2}{2} & 0 & 0 \\ \Delta t & 0 & 0 \\ 0 & \frac{\Delta t^2}{2} & 0 \\ 0 & \Delta t & 0 \\ 0 & 0 & \frac{\Delta t^2}{2} \\ 0 & 0 & \Delta t \end{bmatrix},$$

$$C = \begin{bmatrix} 1 & 0 & 0 & 0 & 0 & 0 \\ 0 & 0 & 1 & 0 & 0 & 0 \\ 0 & 0 & 0 & 0 & 1 & 0 \end{bmatrix}.$$

The disturbance w_t has been introduced to model uncertainties and approximation errors of the UAV model and external disturbances. We assume that $w_t \in \mathbb{W}$, where $\mathbb{W}$ is a known bounded uncertainty set. We denote $\mathbb{X}$ the convex set of feasible states. It can be readily verified that the triple (A, B, C) is reachable and observable.

4.2 MPC reference states and inputs

The sequence of reference states $\tilde{x}_{\{t,...,t+N-1\}}^{[i]}$ of the nominal model is computed implementing in the reference state/inputs sub-module the following dynamic system

$$\begin{bmatrix} \tilde{x}_{t+1}^{[i]} \\ \tilde{e}_{t+1}^{[i]} \end{bmatrix} = \begin{bmatrix} A & 0_{6\times3} \\ -C & I_3 \end{bmatrix} \begin{bmatrix} \tilde{x}_t^{[i]} \\ \tilde{e}_t^{[i]} \end{bmatrix} + \begin{bmatrix} B \\ 0_{3\times3} \end{bmatrix} \tilde{u}_t^{[i]} + \begin{bmatrix} 0_{6\times3} \\ I_3 \end{bmatrix} \tilde{p}_{t+1}^{[i]}, \tag{11}$$

where the new state variable $\tilde{e}_{t+1}^{[i]}$ is the integral of the tracking error $\tilde{p}_{t+1}^{[i]} - C\tilde{x}_t^{[i]}$.

The sequence of reference inputs $\tilde{u}_{\{t,...,t+N-2\}}^{[i]}$ is computed using the control law

$$\tilde{u}_{t+1}^{[i]} = \tilde{K}_x \tilde{x}_{t+1}^{[i]} + \tilde{K}_e \tilde{e}_{t+1}^{[i]}, \tag{12}$$

where the gain $\tilde{K} = \left[\tilde{K}_x \; \tilde{K}_e\right]$ can be designed with any stabilizing algorithm, such as LQ or pole placement.

4.3 MPC optimization problem

In order to implement the robust MPC algorithm proposed in Farina et al. (2014), the tracking module solves at each discrete time instant the following constrained optimization problem

$$\min_{\hat{x}_t^{[i]},\hat{u}^{[i]}_{\{t,\dots,t+N-2\}}} \sum_{j=0}^{N-2} \left\|\hat{x}^{[i]}_{t+j}-\tilde{x}^{[i]}_{t+j}\right\|^2_Q+\left\|\hat{u}^{[i]}_{t+j}-\tilde{u}^{[i]}_{t+j}\right\|^2_R$$
$$+\left\|\hat{x}^{[i]}_{t+N-1}-\tilde{x}^{[i]}_{t+N-1}\right\|^2_P, \quad (13)$$

subject to

$$\hat{x}^{[i]}_{t+1}=A\hat{x}^{[i]}_t+B\hat{u}^{[i]}_t, \quad (14a)$$
$$\hat{x}^{[i]}_{t+j}\in\hat{\mathbb{X}}^{[i]}, \quad \forall j=1,\dots,N-2, \quad (14b)$$
$$x^{[i]}_t-\hat{x}^{[i]}_t\in\varepsilon^{[i]}, \quad (14c)$$
$$C(\hat{x}^{[i]}_{t+j}-\tilde{x}^{[i]}_{t+j})\in\Delta^{[i]}_p, \forall j=1,\dots,N-2, \quad (14d)$$
$$x^{[i]}_{t+N-1}-\hat{x}^{[i]}_{t+N-1}\in\kappa^{[i]}\varepsilon^{[i]}, \quad (14e)$$

The set $\varepsilon^{[i]}$ in (14c) is defined as the robust positively invariant (RPI) set

$$\varepsilon^{[i]}=\bigoplus_{j=0}^{\infty}(A+BK)^j\mathbb{W}^{[i]}, \quad (15)$$

where the gain K must be defined so as to obtain $(A+BK)$ to be Schur stable. In particular, we compute $\varepsilon^{[i]}$ as an outer approximation of the minimum RPI using the method discussed in Rakovic et al. (2005). The set $\hat{\mathbb{X}}^{[i]}$ in (14b) is computed as

$$\hat{\mathbb{X}}^{[i]}=\mathbb{X}^{[i]}\ominus\varepsilon^{[i]}\,. \quad (16)$$

Finally, the set $\Delta^{[i]}_p\subseteq\mathbb{R}^3$ in (14d) and the value $\kappa^{[i]}>0$ in (14e) are tuning parameters.

In the functional cost, the symmetric weighting matrices $Q\geq 0$ and $R>0$ are free design parameters, while P is assumed to satisfy the Lyapunov equation

$$(A+BK)^TP(A+BK)-P=-(Q+K^TRK). \quad (17)$$

From the solution of the optimization problem, we obtain the control inputs for the i-th multi-copter

$$u^{[i]}_t=\hat{u}^{[i]}_{t|t}+K(x^{[i]}_t-\hat{x}^{[i]}_t). \quad (18)$$

5. SYSTEM VALIDATION

To test the developed guidance and control system we have considered the cooperative load transport problem, where a payload is connected by wires to a swarm of UAVs and moved to a final position. A simulator has been developed following the approach described in Tartaglione et al. (2017). In particular, the multi-copters han been modeled with the 6DoF dynamic model (Stevens and Lewis, 2003) and the payload with the 3DoF dynamic model. The constraints of the interconnected system have been computed with the Udwadia-Kalaba equation (Udwadia and Phohomsiri, 2007) and the atmospheric disturbances with the Von Karman wind turbulence model and the discrete wind gust model.

The simulated scenarios were characterized by a swarm of $M=4$ *micro* quad-copters with $m=1.4kg$ and $d_{UAV}=0.3m$, while the payload was assumed to have mass $m_l=0.4kg$. The payload had to be moved from the point $[5.0\ 5.0\ {-14.0}]^T\ m$ to the point $[110.0\ 110.0\ {-4.0}]^T\ m$ in a region characterized by 3D obstacles of different shapes (see Fig. 3). For this application, the virtual leader was assumed to be the payload and the UAVs guidance module had to optimize the payload trajectory. The virtual structure was defined by $l^{[i]}=5.5m$, $\alpha^{[i]}=i\pi/2$ and $\nu^{[i]}=5\pi/12$ for $i=1,\dots,4$.

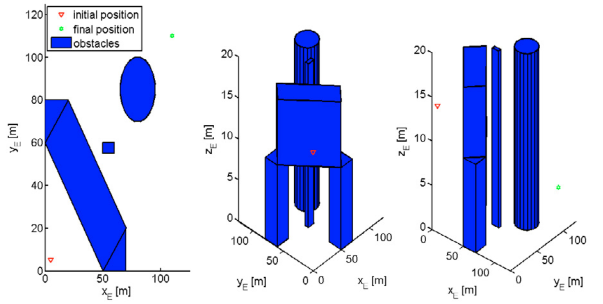

Fig. 3. Simulated scenario.

In order to simulate a real-time implementation we chose $\Delta t=0.5s$ and $\Delta t_{inner}=0.01s$. The free tuning parameters in the trajectory and MPC optimization problems were fixed through a trial and error procedure to obtain satisfying performance in the absence of atmospheric disturbances. In particular, the MPC optimization problem (14) was defined by setting the following parameters. Considering the mission goal and the UAV performance we set $\mathbb{X}^{[i]}=[0.0\ 120.0]\times[-5.0\ 5.0]\times[0.0\ 120.0]\times[-5.0\ 5.0]\times[-20.0\ 0.0]\times[-5.0\ 5.0]$ for $i=1,\dots,4$ (dimension in m and m/s, respectively). For each $i=1,\dots,4$, we set $\mathbb{W}^{[i]}=\mathscr{C}^6(0.02)$, $\Delta^{[i]}_z=\mathscr{C}^3(0.001)$ and $\kappa^{[i]}=1$. The cost function was specified by the length of the prediction horizon $N=10$ and the weighting matrices $Q=I_6$ and $R=180I_3$. Finally, the matrix K was the gain of the LQ regulator with the weighting matrices Q and R. The matrix $\tilde{K}$ used to compute the reference control law (12) was the gain of the LQ regulator with the weighting matrices $\tilde{Q}=I_9$ and $\tilde{R}=2000I_3$. To compute the reference trajectory, the optimization problem (4) was defined setting $\gamma=1$, $T=\text{diag}([10\ 10\ 20])$.

To evaluate the transport mission success, we have checked the payload tracking trajectory error, the obstacle avoidance constraints and the UAVs attitude.

The tracking trajectory error was evaluated considering the payload position

$$E(i)=\left\|p^{[l]}_{t_0+i\Delta t}-\tilde{p}^{[l]}_{t_0+i\Delta t}\right\|. \quad (19)$$

More specifically, we considered the mean of the tracking trajectory error

$$E_{mean}=\frac{1}{N_{tot}}\sum_{i=0}^{N_{tot}}E(i), \quad (20)$$

and the maximum of the tracking trajectory error

$$E_{max}=\max\{E(1),E(2),\dots,E(N_{tot})\}, \quad (21)$$

as performance indexes. In particular, three different atmospheric conditions were simulated: (i) without atmo-

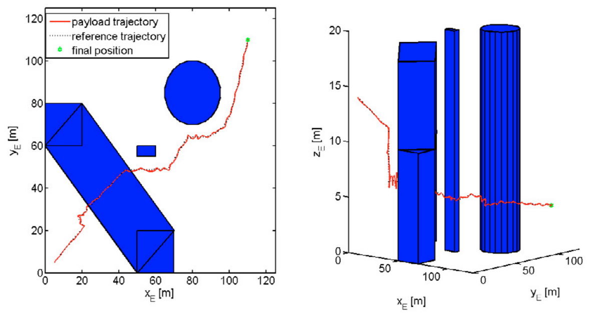

Fig. 4. Payload trajectory: the figures show the reference trajectory and the actual trajectory.

spheric disturbances, we obtained $E_{mean} = 0.431m$ and $E_{max} = 1.628m$; (ii) setting $V_{gust} = [1\ 1\ 0]^T\ m/s$ and $V_{turb} = 3m/s$, we obtained $E_{mean} = 0.592m$ and $E_{max} = 1.575m$; (iii) setting $V_{gust} = [2\ 2\ 0]^T\ m/s$ and $V_{turb} = 6m/s$, we obtained $E_{mean} = 0.853m$ and $E_{max} = 4.134m$. As expected, the performance worsen when increasing the disturbances, but the mission goal is completed.

Below the results of the simulation characterized by $V_{gust} = [1\ 1\ 0]^T\ m/s$ and $V_{turb} = 3m/s$ are shown as an example of the results obtained.

Fig. 4 shows a comparison between the payload trajectory and its reference trajectory. In spite of the UAVs tracking error, the obstacle avoidance constraints was satisfied and the collisions avoided.

6. CONCLUSIONS

In this paper, a decentralized real-time system for the guidance and control of a swarm of multi-copters in a 3D environment has been proposed. Its architecture is based on three different control modules to solve the problems of trajectory planning, trajectory tracking and speed and attitude control.The guidance module computes the UAV reference trajectory as the solution to a constrained optimization problem, then tracking module computes the optimal control law using a MPC algorithm, finally speed and attitude control module is based on PID control systems. To test and validate the proposed scheme we considered the cooperative load transport problem and we developed a simulator of a multi-body slung-load system. The numerical results show the effectiveness of the proposed approach. Further work will consist in implementing the guidance and control system to carry out flight tests.

REFERENCES

Ariola, M., Mattei, M., D'Amato, E., Notaro, I., and Tartaglione, G. (2016). Model predictive control for a swarm of fixed wing UAVs. In *Congress of the International Council of the Aeronautical Sciences, 2016*. ICAS.

Bai, H., Arcak, M., and Wen, J.T. (2011). *Cooperative control design: a systematic, passivity-based approach*. Communication and Control Engineering. Springer-Verlag New York.

Cao, Y., Yu, W., Ren, W., and Chen, G. (2012). An Overview of Recent Progress in the Study of Distributed Multi-Agent Coordination. *IEEE Trans. Ind. Informat.*, 9(1), 427–438.

D'Amato, E., Di Francesco, G., Notaro, I., Tartaglione, G., and Mattei, M. (2015). Nonlinear dynamic inversion and neural networks for a tilt tri-rotor UAV. In *Workshop on Advanced Control and Navigation for Autonomous Aerospace Vehicles, 2015*. IFAC-PapersOnLine.

De Falco, D., Pennestrí, E., and Vita, L. (2009). Investigation of the influence of pseudoinverse matrix calculations on multibody dynamics simulations by means of the Udwadia-Kalaba formulation. *ASCE Journal of Aerospace Engineering*, 22(4), 365–372.

Dong, X., Yu, B., Shi, Z., and Zhong, Y. (2014). Time-Varying Formation Control for Unmanned Aerial Vehicles: Theories and Applications. *IEEE Trans. Control Syst. Technol.*, 23(1), 340–348.

Farina, M., Betti, G., Giulioni, L., and Scattolini, R. (2014). An approach to distributed predictive control for trackingtheory and applications. *IEEE Trans. Control Syst. Technol.*, 22(4), 1558–1566.

Farina, M., Perizzato, A., and Scattolini, R. (2015). Application of distributed predictive control to motion and coordination problems for unicycle autonomous robots. *Robotics and Autonomous Systems*, 72, 248–260.

Klausen, K., Fossen, T.I., and Johansen, T.A. (2014). Suspended load motion control using multicopters. In *IEEE Mediterranean Conf. of Control and Automation*, 1371–1376.

Klausen, K., Fossen, T.I., Johansen, T.A., and Aguiar, A.P. (2015). Cooperative path-following for multirotor UAVs with a suspended payload. In *IEEE Conf. on Control Applications*, 1354–1360.

Lee, T. (2014). Geometric control of multiple quadrotor UAVs transporting a cable-suspended rigid body. In *IEEE Conf. on Decision and Control*.

Lee, T. (2015). Collision avoidance for quadrotor UAVs transporting a payload via Voronoi tessellation. In *IEEE American Control Conference*.

Lewis, M. and Tan, K. (1997). High Precision Formation Control of Mobile Robots Using Virtual Structures. *Autonomous Robots*, 4 (Issue 4), 387–403.

Luo, D., Xu, W., and Wu, S. (2014). UAV formation flight control and formation switch strategy. *Control and Intelligent System*, 42(1), 65–72.

Mahony, R., Kumar, V., and Corke, P. (2012). Multi-rotor aerial vehicles: modeling, estimation, and control of quadrotor. *IEEE Robotics & Automation Magazine*, 19(3), 20–32.

Murray, R. (2007). Recent research in cooperative control of multivehicle systems. *Journal of Dynamic Systems, Measurement and Control, Transactions of the ASME*, 129 (Issue 5), 571–583.

Nguyen, H. (2014). *Constrained control of uncertain, time-varying, discrete-time Systems: An interpolation-based approach*. Lecture Notes in Control and Information Sciences. Springer International Publishing.

Oriolo, G., De Luca, A., and Vendittelli, M. (2002). WMR control via dynamic feedback linearization: design, implementation, and experimental validation. *IEEE Trans. Control Syst. Technol.*, 10(6), 835–852.

Pascarella, D., Venticinque, S., Aversa, R., Mattei, M., and Blasi, L. (2015). Parallel and distributed computing for UAVs trajectory planning. *Journal of Ambient Intelligence and Humanized Computing*, 6 Issue 6, 773–782.

Paul, T., Krogstad, T.R., and Gravdahl, J.T. (2008). UAV Formation Flight using 3D Potential Field. In *IEEE Mediterranean Conf. on Control and Automation*.

Rakovic, S.V., Kerrigan, E.C., Kouramas, K.I., and Mayne, D.Q. (2005). Invariant Approximations of the Minimal Robust Positively Invariant Set. *IEEE Trans. Autom. Control*, 50 Issue 3, 406–410.

Stevens, B. and Lewis, F. (2003). *Aircraft control and simulation, 2nd Edition*. Mechanical Engineering. Wiley-Interscience.

Tartaglione, G., D'Amato, E., Ariola, M., Salvo Rossi, P., and Johansen, T.A. (2017). Model predictive control for a multi-body slung-load system. *Robotics and Autonomous Systems*, 92.

Udwadia, F. and Phohomsiri, P. (2007). Explicit Poincaré equations of motion for general constrained systems, Part I. Analytical results. *Proceedings: Mathematical, Physical and Engineering Sciences*, 463(2082), 1421–1434.